

Somatomotor-visual resting state functional connectivity increases after 2 years in the UK Biobank longitudinal cohort

Anton Orlichenko^{D, a,*} Kuan-Jui Su,^b Hui Shen,^b Hong-Wen Deng,^b and Yu-Ping Wang^a

^aTulane University, Department of Biomedical Engineering, New Orleans, Louisiana, United States

^bTulane University, School of Medicine, Center for Biomedical Informatics and Genomics, New Orleans, Louisiana, United States

ABSTRACT. **Purpose:** Functional magnetic resonance imaging (fMRI) and functional connectivity (FC) have been used to follow aging in both children and older adults. Robust changes have been observed in children, in which high connectivity among all brain regions changes to a more modular structure with maturation. We examine FC changes in older adults after 2 years of aging in the UK Biobank (UKB) longitudinal cohort.

Approach: We process fMRI connectivity data using the Power264 atlas and then test whether the average internetwork FC changes in the 2722-subject longitudinal cohort are statistically significant using a Bonferroni-corrected *t*-test. We also compare the ability of Power264 and UKB-provided, independent component analysis (ICA)-based FC to determine which of a longitudinal scan pair is older. Finally, we investigate cross-sectional FC changes as well as differences due to differing scanner tasks in the UKB, Philadelphia Neurodevelopmental Cohort, and Alzheimer's Disease Neuroimaging Initiative datasets.

Results: We find a 6.8% average increase in somatomotor network (SMT)-visual network (VIS) connectivity from younger to older scans (corrected $p < 10^{-15}$) that occurs in male, female, older subject (>65 years old), and younger subject (<55 years old) groups. Among all internetwork connections, the average SMT-VIS connectivity is the best predictor of relative scan age. Using the full FC and a training set of 2000 subjects, one is able to predict which scan is older 82.5% of the time using either the full Power264 FC or the UKB-provided ICA-based FC.

Conclusions: We conclude that SMT-VIS connectivity increases with age in the UKB longitudinal cohort and that resting state FC increases with age in the UKB cross-sectional cohort.

© 2024 Society of Photo-Optical Instrumentation Engineers (SPIE) [DOI: [10.1117/1.JMI.11.2.024010](https://doi.org/10.1117/1.JMI.11.2.024010)]

Keywords: fMRI; functional connectivity; UK Biobank; longitudinal; cross-sectional; aging

Paper 23240GR received Aug. 21, 2023; revised Jan. 26, 2024; accepted Mar. 29, 2024; published Apr. 12, 2024.

1 Introduction

Functional magnetic resonance imaging (fMRI) is a noninvasive technique that has proven indispensable for investigating human neural processes *in vivo*.¹ For example, it has been used to

*Address all correspondence to Anton Orlichenko, aorlichenko@tulane.edu

localize the areas associated with vision,² attention,^{3,4} emotion,⁵⁻⁷ and language⁸ to specific regions in the cortex or at least find the regions that are most significantly involved in a specific task. Functional connectivity (FC) is a quantity derived from fMRI that measures the time correlation of the blood oxygen level-dependent (BOLD) signal among different regions in the brain.⁹ FC has recently been used to predict age,^{10,11} sex,^{12,13} race,¹⁴ psychiatric disease status,^{15,16} and preclinical Alzheimer's disease.¹⁷ Efforts to predict general fluid intelligence, although common,^{13,18} are thought by some to be confounded by differential achievement score distribution among ethnicities and the strong presence of race signal in FC.¹⁴ FC has proven effective in predictive studies because of its simplicity and its robust representation of the complex BOLD signal activity as evidenced by high subject identifiability across different scanner tasks and across time.¹⁹⁻²¹

In addition to being used as a predictive tool, FC has been observed to undergo changes throughout the lifespan. For example, connectivity in young children is generally very high among all brain regions and decreases while becoming more modularized during and after puberty.²² The FC of males and females is also quantitatively different, with females having higher intra-default mode network (DMN) connectivity and males having relatively greater connectivity between the DMN and other networks, although there is a wide degree of individual variation.^{23,24} Meanwhile, studies have shown that changes occur in the DMN during late middle and old age,²⁵ although the exact direction of change in FC does not always appear constant.²⁶ In addition, various studies have examined age-related changes in the cingulum²⁷ and medial temporal lobe.²⁸ Given the recent interest in using fMRI to predict preclinical Alzheimer's disease,^{17,26} we believe that a knowledge of ordinary changes in FC during old age is essential. This is especially true because it has been shown that a confounder can easily be mistaken for a true signal indicative of, e.g., general fluid intelligence or achievement score.¹⁴

This study uses the longitudinal cohort of the UK Biobank (UKB)²⁹ to examine changes in the FC of individuals after an average of 2 years, the time between longitudinal scans. The UKB population of subjects with fMRI scans is predominantly (98%) Caucasian, ruling out race as a possible confounding effect. In addition, we investigate changes in FC in longitudinal subpopulations based on subject age and sex. We find that the average FC between somatomotor network (SMT)-visual network (VIS) increases on average from the first scan to the second and that SMT and VIS-related connectivities are more predictive of scan age than those of other networks. The complete FC, or a large subset, is still required to attain the best accuracy.

2 Methods

We first describe the UKB dataset and the longitudinal subset used for our analysis. We then describe preprocessing of the fMRI data and conversion into FC. Finally, we discuss the prediction of older versus younger scans in the longitudinal cohort and detail our methods for analysis of FC changes.

2.1 UKB Longitudinal Cohort

The UKB contains various data of more than 500,000 subjects in the United Kingdom, of whom more than 40,000 have fMRI scans.²⁹ We processed two longitudinal resting state scans for 2722 subjects, taken ~2 years apart. These subjects are approximately equally split between male and female and have significant numbers of younger and older adults. The longitudinal cohort is composed of 1289 genetic males and 1369 genetic females, with the rest not having genetic sex information. The ethnicity of the subset of the UKB with fMRI scans is 98% Caucasian. In addition to the 2722 subjects that we processed, an additional 154 subjects have the second longitudinal scan but not the first, resulting either from missing original source data or a failure in our SPM12-based preprocessing pipeline. In addition, we perform analysis on the UKB working scanner task,^{30,31} which includes a total of 2360 longitudinal subjects, compared with the 2722 subjects having resting state longitudinal scans.

2.2 fMRI Preprocessing

The original scan acquisition parameters are described elsewhere^{30,32} but consist of both resting state and task fMRI scans with a repetition time of TR = 0.735 sec. All resting state

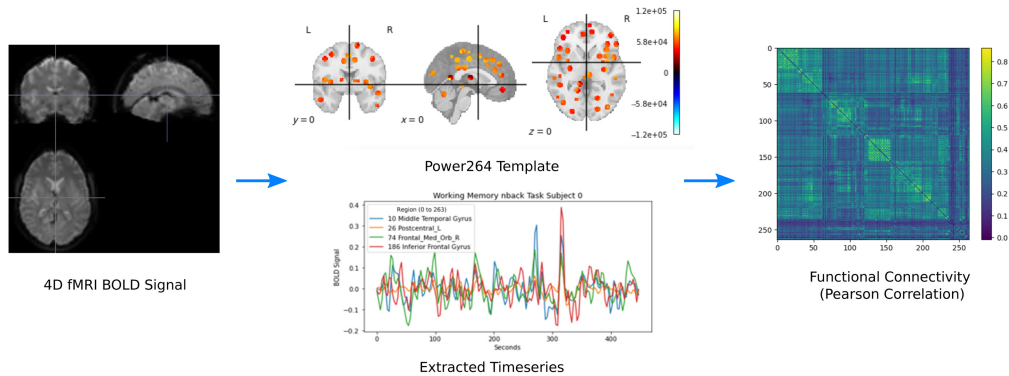


Fig. 1 Preprocessing pipeline for converting 4D fMRI volumes into FC using the Power264 atlas.³⁴ Reproduced with permission from Orlichenko et al.³⁵

four-dimensional (4D) fMRI volumes were processed with SPM12, including coregistration and warping to MNI space.³³ The BOLD signal was extracted using the Power264 atlas,³⁴ which consists of 264 regions of interest (ROIs) grouped into 14 functional networks, with the ROIs represented by 5-mm radius spheres. The resulting time series were bandpass filtered between 0.01 and 0.15 Hz to remove scanner drift, noise, heartbeat, and some breathing signal. The Pearson correlation of the filtered time series was used to create subject-specific FC matrices, which were reduced to the 34,716 unique entries in the upper right triangle and vectorized. The entire procedure is summarized in Fig. 1.

In contrast to the Power264 atlas-derived FC constructed by us, the original UKB data provided the unique part of 21-region and 55-region FC and partial correlation (PC)-based connectivity matrices based on independent component analysis (ICA) in a vectorized format.³⁰ These matrices were calculated through the use of principal component analysis on whole cohort fMRI data followed by ICA,³⁰ meaning that regions overlap in an unpredictable way and are not associated with specific functional networks. Although prediction using 55-component ICA-based FC and PC is often as good as and sometimes better than prediction using Power264 atlas-derived FC, the resulting connectivities are uninterpretable with regard to the BOLD signal within specific regions. In addition, in predicting which scan is older, Power264 asymptotes to a higher predictive accuracy than either of the ICA-derived measures (see Fig. 4).

2.3 Prediction of Scan Order and Analysis of FC

The prediction of the scan age in the UKB longitudinal cohort was carried out by logistic regression³⁶ models with 20 bootstrapping repetitions, using the scikit-learn implementation.³⁶ The regularization parameter was fixed to $C = 1$, which was found to be near the optimal value for all training set sizes using grid search. Prediction was carried out using the difference of vectorized FC matrices as input features and the scan order (younger scan minus older [0] or older scan minus younger [1]) as the prediction target. It was found that a simple difference of the two longitudinal scan FCs gave the best prediction results compared with concatenation or difference and concatenation, using either logistic regression or a multi-layer perceptron. The training set was created with randomization of whether the older scan was subtracted from the younger scan or the younger scan was subtracted from the older scan. The predictive ability was tested at various training set sizes, from 50 to 2000 subjects, with the remaining subjects forming the test set. In addition to the resting state scanner task, we have repeated this analysis for the UKB working scanner task, a faces/shapes emotion identification task.^{30,31} We also include a comparison with average FC differences due to different scanner tasks as found in the widely used Philadelphia Neurodevelopmental Cohort (PNC) dataset,³⁷ computing the mean FC differences for combinations of scanner tasks (resting state, working memory, or emotion identification). Our code for computing prediction accuracy can be found online (<https://github.com/aorliche/ukb-longitudinal-smt-vis>). However, the UKB data sharing policy precludes us from posting the longitudinal data itself; interested researchers may contact us with any questions.

The analysis of FC was performed by finding the mean (Fig. 2) and standard deviation (Fig. 10) of the older scan FC minus the younger scan FC for the longitudinal cohort. In addition,

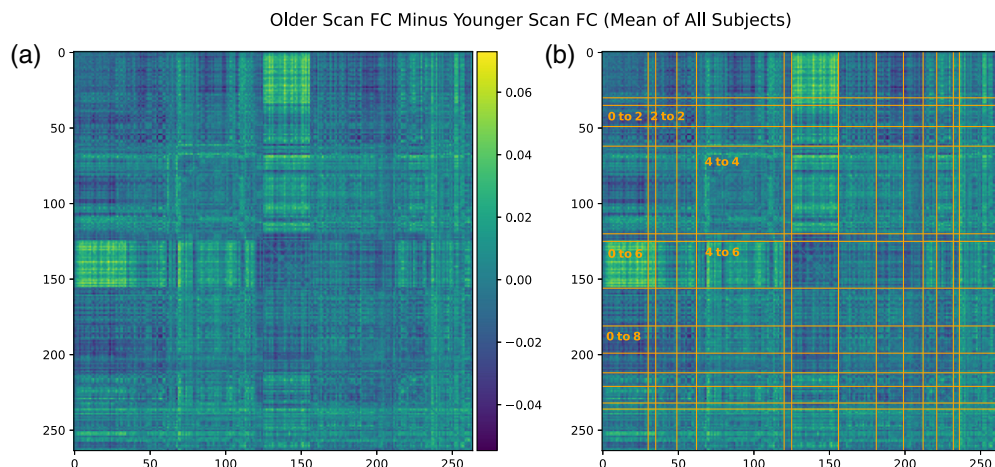


Fig. 2 Difference in FC calculated by the older scan minus the younger scan, averaged over all 2722 longitudinal cohort subjects. There are significant average differences in SMT–VIS connectivity (labeled 0 to 6). The same plot is displayed on panels (a) and (b), with Power264 network divisions on panel (b). Network labels are given in Table 1.

the prediction of the scan order was carried out using the average connectivity among the Power264 networks, in which each network consisted of many individual ROIs. As before, logistic regression with 20 bootstrap repetitions and $C = 1$, with 2000 subjects in the training set and the rest in the test set, was used for this purpose. A Bonferroni-corrected two-sided t -test was applied to the 105 average internetwork connectivity differences (from the complete graph of 14 functional networks) of the 2722 longitudinal subjects to determine if they were significantly different from zero (Fig. 5b). Finally, we examine changes in FC in the UKB cross-sectional cohort, which contains 23,672 younger (<55 years old) and older (>65 years old) male and female subjects, also using a two-sided t -test with p -values adjusted by Bonferroni correction.

3 Results

We first describe trends in FC changes during the 2 years or more between longitudinal scans, summarize the ability of simple machine learning models to identify older versus younger scans, and investigate the ability of specific internetwork connectivities to predict the scan order. We then summarize the statistical significance of internetwork FC changes with aging, in both the longitudinal and cross-sectional cohorts of the UKB. Next, we consider the possibility that the observed longitudinal changes are due to a change in the scanner task by presenting inter-task FC differences in the PNC dataset.³⁷ Finally, we confirm the presence of increased longitudinal SMT–VIS connectivity in the UKB working task scan in addition to the UKB resting state scan.

3.1 Internetwork FC Changes

In Fig. 2, we show that, on average, SMT–VIS connectivity increases from younger to older scans. Figure 2(b) displays divisions of the 14 functional networks included in the Power264 atlas. Network labels and abbreviations are listed in Table 1. The increase in connectivity is large and distinct over the majority of SMT–VIS FCs compared with other non-SMT and non-VIS FCs. Many FCs involving the VIS appear to increase in connectivity from the first scan to the second. The average change in FC in the SMT–VIS connection is 6.8%, corresponding to a mean change $\mu_{\Delta\rho} = +0.03$, compared with a standard deviation of $\sigma_{\Delta\rho} = 0.26$. Figure 5 shows that, due to the large number of subjects, this difference is very statistically significant. Figure 3 displays the same analysis, i.e., the average FC change from the first scan to the second, for four subsets of the cohort. These subsets are male, female, young (<55 years old), and old (>65 years old) subjects. All four subsets showed the same patterns of changes in FC as the whole cohort; thus, we rule out very old age or gender as confounding factors.

Table 1 Regions, abbreviations, and labels in the Power264 atlas.

Functional networks					
Label	ROIs		Label	ROIs	
0	0 to 29	Somatomotor hand (SMT)	7	156 to 180	Frontoparietal (FRNT)
1	30 to 34	Somatomotor mouth (SMT)	8	181 to 198	Salience (SAL)
2	35 to 48	Cinguloopercular (CNG)	9	199 to 211	Subcortical (SUB)
3	49 to 61	Auditory (AUD)	10	212 to 220	Ventral attention (VTRL)
4	62 to 119	Default mode (DMN)	11	221 to 231	Dorsal attention (DRSL)
5	120 to 124	Memory (MEM)	12	232 to 235	Cerebellar (CB)
6	125 to 155	Visual (VIS)	13	236 to 263	Uncertain (UNK)

**Fig. 3** Significant increase in SMT–VIS connectivity after an average of 2 years in the UKB longitudinal cohort appears in male, female, younger, and older groups and seems to be an invariant feature of FC change in the longitudinal UKB cohort.

3.2 Predicting Older Scan of Pair

In Fig. 4, one can see that it is possible to predict which scan of a longitudinal pair is older with the Power264 atlas at an accuracy of 82.5%, having 2000 subjects in the training set and the rest in the test set. This measurement was repeated with 20 bootstrap iterations and averaged. The entire 34,716-feature upper right triangle of the FC matrix was used to make the prediction. One can also see that the ICA FC/PC matrices provided preprocessed by the UKB curators along with

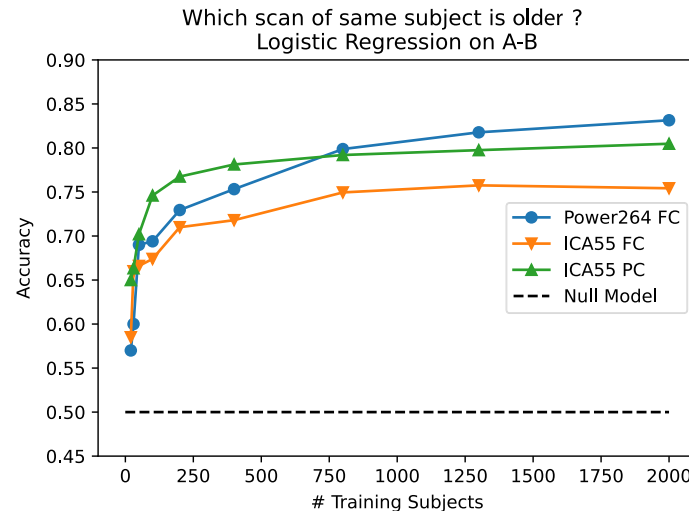


Fig. 4 Capability of predicting the older scan of a pair based on the difference of FC between the two scans as a function of the number of training subjects. Three inputs are used: 55 component ICA FC, 55 component ICA PC, and the Power264 atlas FC. Prediction accuracy as displayed is on the test set, not the training set, and asymptotes are at 82.5%.

the UKB data are also able to predict the scan order, although at a slightly reduced accuracy. Prediction is possible at an accuracy of 60% to 70% using only 100 to 200 training set subjects. This shows an expected dependence of accuracy of the test set prediction of the scan order on the training set size. Note that most machine learning models will perform better on the training set than the test set. Overfitting, in which the prediction accuracy is high on the training set but close to or worse than the null model (50%) on the test set, is not observed.

3.3 Prediction of Older Scan Using Specific Internetwork Connections

In Fig. 5, we rank average internetwork FCs in their ability to predict the scan order. As expected from the mean change in FC (Fig. 2), the SMT–VIS connection is the most predictive of longitudinal scan age. Furthermore, SMT and VIS are included among the next several most predictive internetwork connections. In Fig. 5b, we plot the predictive ability of all 105 internetwork connections, along with a *p*-value for the internetwork FC change being significantly different from zero. The raw *p*-value was multiplied by 105 to account for multiple comparisons. It is highly significant for the first 10 or so most predictive internetwork connections, and we find a *p*-value of $p < 10^{-15}$ for the increase in SMT–VIS connectivity from the first longitudinal scan to the second. For reference, Fig. 6 displays the ROIs making up the SMT and VIS networks in the Power264 atlas.

Table 2 lists the number of subjects whose FC increased or decreased for the SMT–VIS connection and over the entire brain connectome. The table is divided among the four subsets of the longitudinal cohort mentioned previously. In addition, we correlated several dozen subject phenotypes, longitudinally tracked variables with changes in FC, and report the most significant in Appendix B. In that section, we find an interesting but small correlation with hand grip strength, body mass index (BMI), and basal metabolic rate. In Sec. 3.4, we find that average resting state FC increases with age across most internetwork connections in the much larger UKB cross-sectional cohort.

3.4 FC Changes with Age in the UKB Cross-Sectional Cohort

We find that average resting state FC has a significant increase in almost all internetwork connections in the UKB cross-sectional cohort. Average maps of the FC change are shown in Fig. 7. We fail to find a higher SMT–VIS change as compared with other connections; however, almost all internetwork regions have a large positive change in FC with aging. We give precise numbers for four internetwork connections as well as total FC in Table 3. In total, there are 9387 older males (>65 years old), 2425 younger males (<55 years old), 8728 older females (>65 years old), and 3132 younger females (<55 years old) in the UKB cross-sectional cohort.

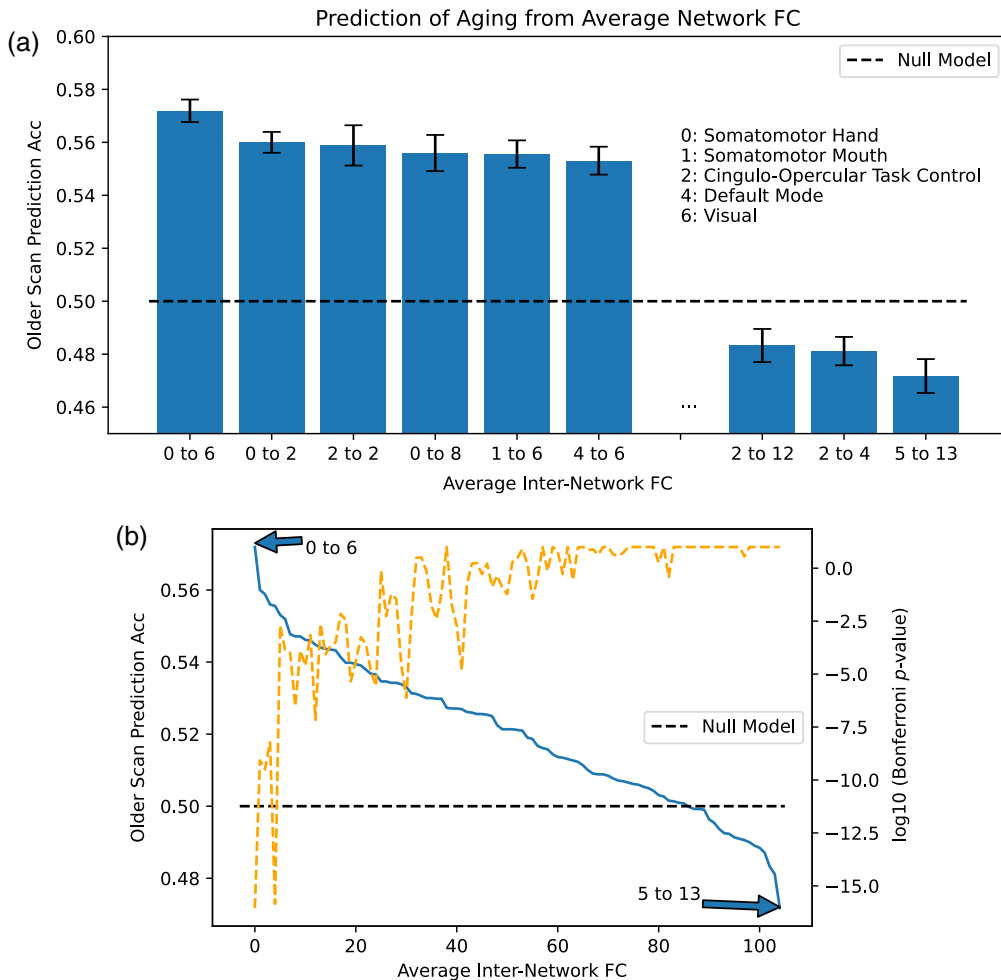


Fig. 5 Ability to predict which scan of a subject is older based on average connectivity among regions. (a) Best and worst internetwork connectivities for prediction. (b) Prediction accuracy for all 105 internetwork connectivities. We find that SMT–VIS connectivity has the maximum predictive ability of all regions at 57%. In general, network-level connectivities involving SMT and VIS networks have higher predictive ability compared with other regions. The dashed orange line displays log base 10 of the Bonferroni-corrected p -value for significance of FC change between scans. Note that the Bonferroni-corrected p -value for the observed SMT–VIS connectivity increase is $p < 10^{-15}$.

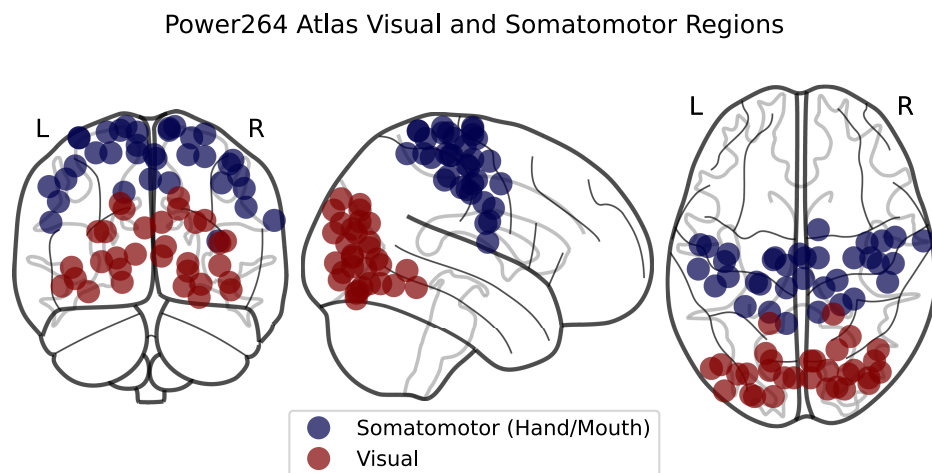
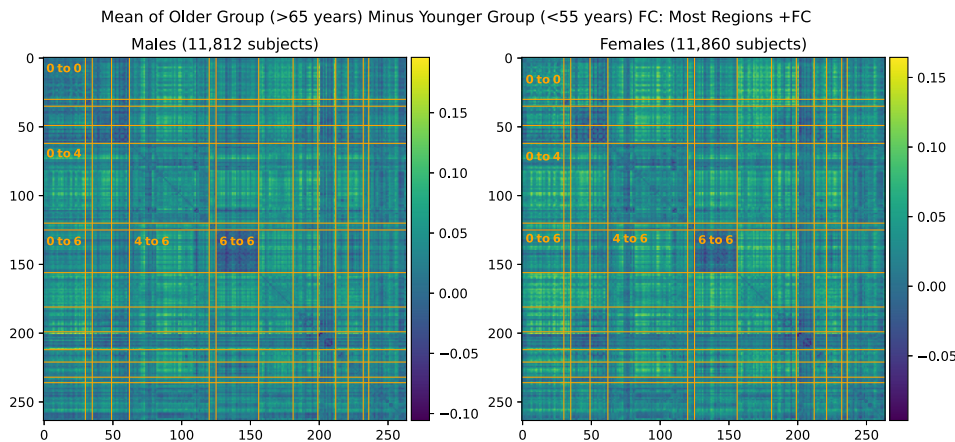


Fig. 6 SMT and VIS regions in the Power264 atlas.

Table 2 Number of subjects in the longitudinal cohort increasing and decreasing in average FC within the SMT–VIS connection and within the whole brain.

Group	+SMT–VIS FC	–SMT–VIS FC	+Total FC	–Total FC	Total subjects
Male	778 (60.4%)	511	690 (53.5%)	599	1289
Female	741 (54.1%)	628	671 (49.0%)	698	1369
<55 years old	269 (59.0%)	187	249 (54.6%)	207	456
>65 years old	577 (56.5%)	445	520 (50.1%)	502	1022

**Fig. 7** Mean FC change from the younger to older group in the large UKB cross-sectional cohort.**Table 3** Average FC changes with aging in the UKB cross-sectional cohort from young subjects (<55 years old) to old subjects (>65 years old).

Regions	Male (young to old)			Female (young to old)		
	FC increase	Std dev of avg FC	p-Value	FC increase	Std dev of avg FC	p-Value
SMT–VIS (0 to 6)	0.031	0.13	<10 ⁻²³	0.029	0.13	<10 ⁻²⁵
SMT–DMN (0 to 4)	0.045	0.11	<10 ⁻⁷⁸	0.043	0.11	<10 ⁻⁸²
DMN–VIS (4 to 6)	0.042	0.11	<10 ⁻⁶⁰	0.035	0.11	<10 ⁻⁵²
VIS–VIS (6 to 6)	-0.014	0.10	<10 ⁻⁷	-0.009	0.11	<0.002
Total FC	0.035	0.09	<10 ⁻⁶⁴	0.031	0.087	<10 ⁻⁶²

SMT, somatomotor network; VIS, visual network; DMN, default mode network; FC, functional connectivity

3.5 Comparison with FC Differences among Scanner Tasks in the PNC Dataset

We consider the possibility that the difference in SMT–VIS connectivity between the two scans of the longitudinal cohort is due to a change in the scanner task. In Fig. 8, we show the average FC differences among three different tasks in the PNC dataset.³⁷ This dataset contains 1345 children and young adults having all of three different scanner tasks: resting state, working memory, and emotion identification. The preprocessing and FC creation steps for this dataset have been described elsewhere.¹⁰ We note that VIS–VIS connectivity has the greatest average difference among different tasks and that the change in SMT–VIS connectivity is not more qualitatively different than for other internetwork connections. Also, the magnitude of change in FC in the PNC dataset among tasks is much larger than in the UKB longitudinal cohort. We observe a

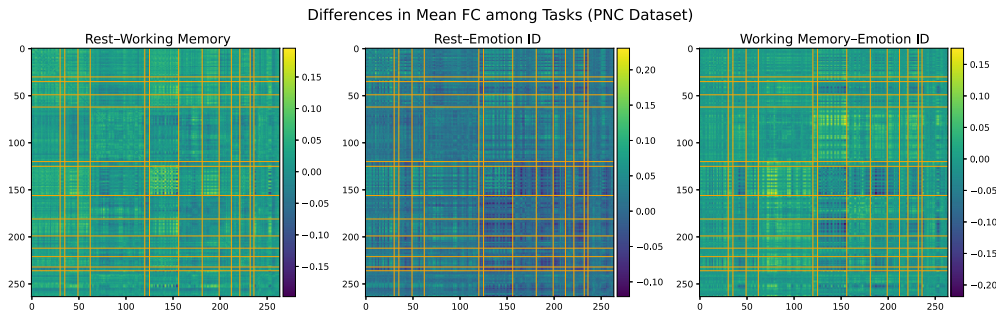


Fig. 8 Average differences in FC among three scanner tasks of 1345 subjects in the PNC dataset. This is a cross-sectional, not longitudinal, dataset.

$\Delta\rho = 0.03$ average change in SMT–VIS connectivity in the UKB longitudinal cohort compared with a $\Delta\rho > 0.05$ average FC change in some internetwork connections among different scanner tasks in the PNC dataset.

3.6 Validation on UKB Working Task

In addition to the resting state scanner task, the UKB had fMRI scan participants undergo a face/shape emotion identification task.^{30,31} As validation for the findings of increased SMT–VIS connectivity in resting state scan data, we performed the same analysis described previously for the resting state scanner task on the longitudinal cohort working task scan. The number of subjects

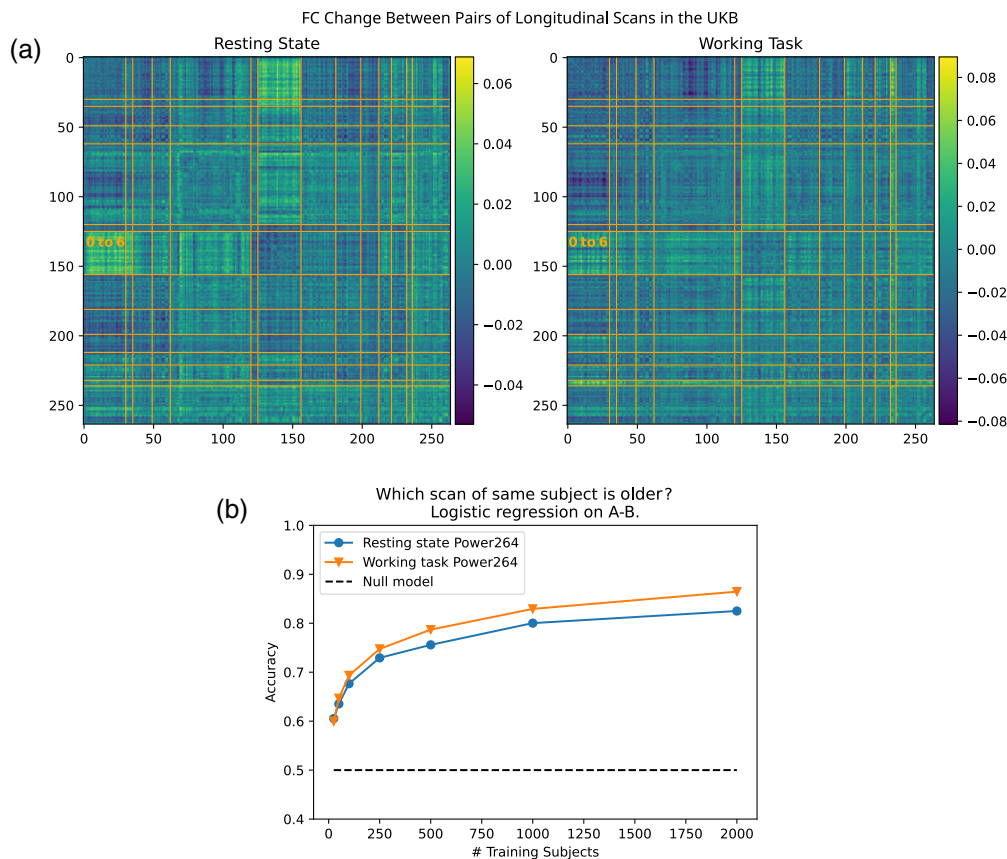


Fig. 9 (a) Comparison of resting state with working task average FC change in the longitudinal cohort. We see qualitatively the same pattern, with the high SMT–VIS connectivity change along with the high change for other VIS-connected FCs. (b) Ability to predict which of a scan pair from a single subject was older, using resting state and working task FC data. We find that it is slightly easier to predict the scan age in the longitudinal cohort using the working scanner task than the resting state scanner task.

with the working scanner task was smaller than for the resting state, with 2360 working task subjects compared with 2722 resting state task subjects. As shown in Fig. 9(a), one can see the same qualitative pattern of FC changes in the working task as in the resting state task. In addition, Fig. 9(b) shows that the working state FC can predict which scan is older at least as well as the resting state FC.

4 Discussion

Farràs-Permanyer et al.³⁸ found that mean resting state FC may increase throughout the entire brain for the oldest subject (>80 years old) group. In another study, Hafkemeijer et al.³⁹ found that resting state FC increases in older adults with memory complaints. As shown in Appendix A, we confirm a small, statistically insignificant increase in total longitudinal FC in the healthy controls of the Alzheimer's Disease Neuroimaging Initiative (ADNI) dataset,⁴⁰ another elderly population with multiple longitudinal fMRI scans. In Sec. 3.4, we show that there is a large, statistically significant increase in average resting state FC across almost all internetwork connections in the UKB cross-sectional cohort with increased age. This cross-sectional cohort is much larger than the longitudinal cohort that we describe in the main part of this paper. The fact that SMT–VIS FC also increases in the cross-sectional cohort, but not disproportionately compared with the rest of FC, raises the possibility of a change in resting state scanner task during the second longitudinal scan. The credence given to this possibility should be reduced because we find a similar increase in the UKB longitudinal cohort working task, as described in Sec. 3.6. We believe that this longitudinal change is not an artifact of our preprocessing methods. Confidence should increase in our preprocessing methods because the UKB-provided ICA-based FC and PC is also able to predict longitudinal scan ordering at almost the same level as our Power264-based approach, although the ICA FC and PC matrices are not interpretable.

Many studies have focused on examining connectivity in the DMN associated with aging.^{41,42} These studies found areas of increased connectivity and areas of decreased connectivity. There are two problems with such studies. First, they are for the most part cross-sectional and do not follow a single subject across a multiyear period. Second, they mostly use small numbers of subjects, with the majority of studies enrolling fewer than 50, making it impossible to identify small effects. On the other hand, one study performed on a cohort of more than 2000 older subjects in Rotterdam found age-related changes in connectivity to be complicated, drawing no firm conclusions.⁴³ We note that the Rotterdam study was not longitudinal but cross-sectional.

We conjecture that most studies only focused on DMN and reported that decreased connectivity⁴¹ in aging populations may be related to the large number of ROIs in the DMN and an implicit bias inherent in the word “connectivity.” Naturally, as we reach very old age, we expect physical connections to degenerate, not become stronger. In fact, FC is really the synchronization of the BOLD signal among regions and does not imply a direct physical link among regions. Young children are known to have higher average FC than young adults;^{22,44} thus, older subjects may be seen as reverting to a less optimal state as they age.

On the other hand, as we describe in Appendix B, physical observables such as hand grip strength in the UKB longitudinal cohort are weakly correlated with an increase in FC in SMT–cerebellar (CB) and VIS–CB connectivity. In addition, we find that BMI and basal metabolic rate are weakly correlated with the longitudinal increase in SMT–VIS connectivity (see Appendix B). This may suggest a small health-related effect that is found throughout the study cohort and includes male, female, younger, and older subjects.

We show in this work that the average connectivity increase in the SMT–VIS connection is small but highly statistically significant. The average change in FC in this connection is only 6.8%, corresponding to a mean change $\mu_{\Delta\rho} = +0.03$, compared with a standard deviation of change from subject to subject of $\sigma_{\Delta\rho} = 0.26$ (see Fig. 10). However, using our longitudinal sample of 2722 subjects, we find that the average SMT–VIS connectivity change from younger to older scans is very significant after Bonferroni correction for multiple comparisons (Fig. 5). Finding such small effects is helped by the use of a large number of subjects and longitudinal data.

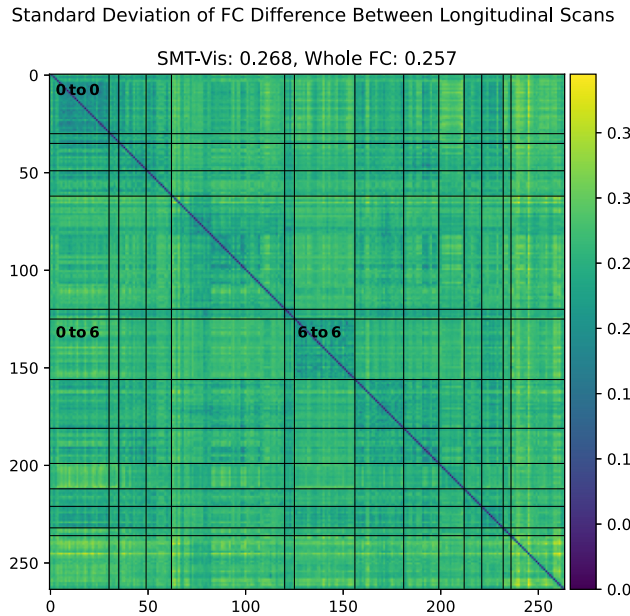


Fig. 10 Standard deviation of the difference between older and younger scan FCs in the UKB longitudinal cohort. Note that the magnitude of average standard deviation (0.26) of SMT–VIS connectivity change is larger compared with mean SMT–VIS connectivity change (0.03). However, we show in Fig. 5 that this connectivity change is highly statistically significant. The smallest average standard deviations are found in SMT–SMT (0.2) and VIS–VIS (0.22) connectivities.

5 Conclusion

In this work, we preprocessed a 2722 subject longitudinal subset of the UKB dataset and examined FC using the Power264 atlas. We found that, in scans taken an average of 2 years apart, the average FC between SMT and VIS regions tended to increase at a Bonferroni-corrected p -value of $p < 10^{-15}$. This occurred in male, female, younger (<55 years old), and older (>65 years old) subject groups. We verified the ability of this average FC increase to predict scan ordering using simple machine learning models. The identification of an increase in connectivity with nonpathological aging, in longitudinal as well as cross-sectional cohorts, and specifically in the SMT–VIS synchronization of the BOLD signal, may lead to novel insights about brain function in old age. The identified increase in SMT–VIS connectivity with aging could also appear as a confounder in future studies of dementia or neurodegenerative diseases and should be guarded against. Finally, we rule out the possibility of a change in scanner task leading to the identified increase in resting state SMT–VIS connectivity by finding a similar increase in SMT–VIS connectivity in the UKB longitudinal working scanner task.

6 Appendix A: Longitudinal FC Changes in the ADNI Dataset

We examined the longitudinal change in FC of healthy controls in the ADNI dataset⁴⁰ [age matched subjects who do not develop Alzheimer’s disease (AD) pathology]. We used scans taken an average of 1 year apart. We confirmed a small, statistically insignificant increase in total FC but fail to find the same SMT–VIS increase relative to the rest of FC as in the UKB. Statistics are given in Table 4, and the average FC change is shown in Fig. 11.

Table 4 There is a small but positive change in FC in ADNI healthy controls (subjects who do not go on to develop AD).

Average FC increase	Std dev FC change	+Total FC	-Total FC	Total subjects
0.015	0.131	184 (52.7%)	165	394

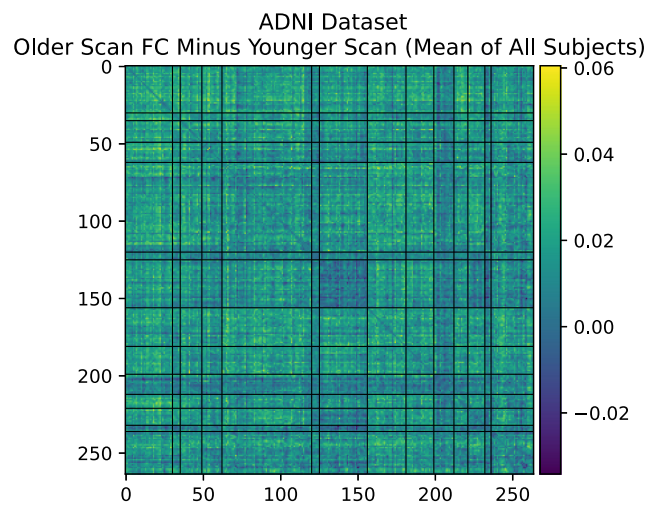


Fig. 11 Mean longitudinal changes in FC between first and second scans in healthy controls of the ADNI dataset.

7 Appendix B: Correlation of Change in FC with Longitudinal Outcomes in the UKB

We identified several correlations between longitudinal change in FC and changes in clinical outcomes associated with the two scan timepoints in the UKB dataset. These, along with the

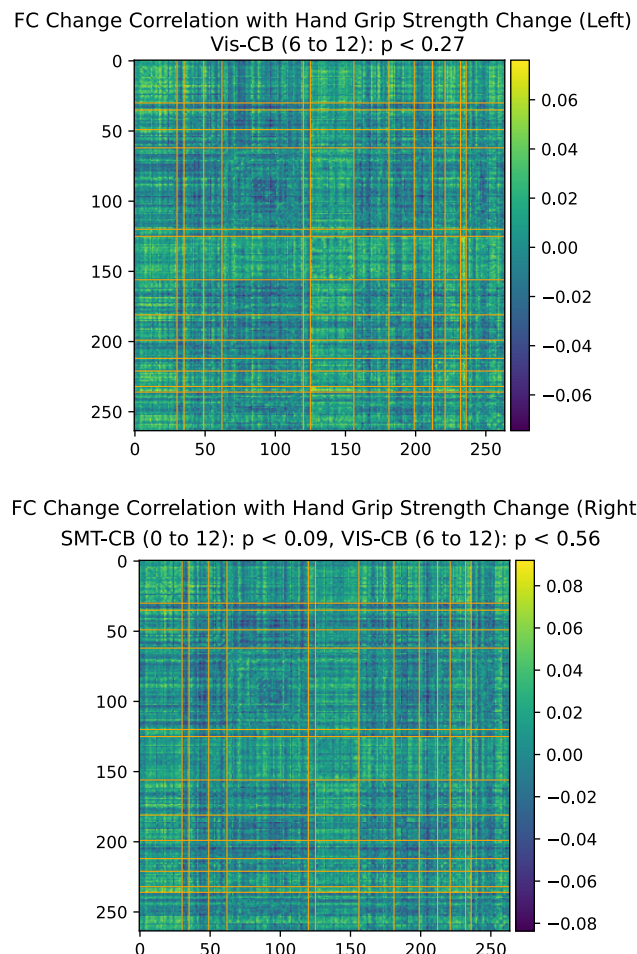


Fig. 12 Hand grip strength change association with FC change in the longitudinal cohort. Bonferroni-corrected p -values.

UKB field identifiers of the outcomes, are presented below. All p -values are Bonferroni-corrected with $n = 105$ multiple comparisons (one for each average internetwork connectivity).

7.1 SMT Hand, VIS, and CB Connectivity and Grip Strength (f.46.2.0, f.46.3.0, f.47.2.0, f.47.3.0)

We find a marginally significant association between the change in hand grip strength and VIS–CB and SMT–CB connectivity change (Fig. 12).

7.2 BMI and Basal Metabolic Rate (f.23104.2.0, f.23104.3.0, f.23105.2.0, f.23105.3.0)

We find a not statistically significant but suggestive association between BMI and basal metabolic rate change and SMT–VIS connectivity change (Fig. 13).

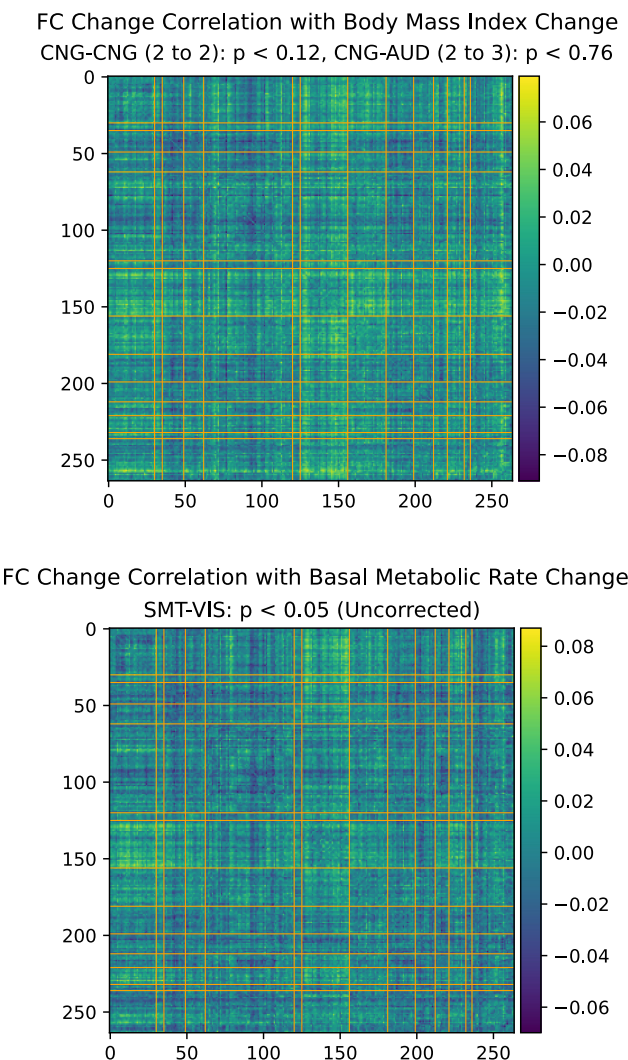


Fig. 13 BMI and basal metabolic range change association with FC change in the longitudinal cohort. Bonferroni-corrected p -values.

Disclosures

The authors have no conflicts of interest to report.

Code and Data Availability

fMRI and phenotype data came from the UKB (application ID 61915), available via application to qualified researchers. Additional data used in [Appendix A](#) came from the ADNI, available via application from <https://adni.loni.usc.edu/>. Further neuroimaging data were acquired from the Neurodevelopmental Genomics: Trajectories of Complex Phenotypes database of genotypes and phenotypes repository, dbGaP Study Accession ID phs000607.v3.p2. All code used in this study is available from GitHub at <https://github.com/aorliche/ukb-longitudinal-smt-vis>. We do not have permission to post original subject data; however, it may be obtained via application from the sources listed above.

Acknowledgments

The authors would like to acknowledge the National Institutes of Health (NIH) (Grant Nos. R01 GM109068, R01 MH104680, R01 MH107354, P20 GM103472, R01 EB020407, R01 EB006841, and R56 MH124925) and the National Science Foundation (NSF) (Grant No. 1539067) for partial funding support. This research was supported in part using high-performance computing resources and services provided by Information Technology at Tulane University, New Orleans, Los Angeles.

References

1. J. W. Belliveau et al., “Functional mapping of the human visual cortex by magnetic resonance imaging,” *Science* **254**(5032), 716–719 (1991).
2. D. D. Cox and R. L. Savoy, “Functional magnetic resonance imaging (fMRI) “brain reading”: detecting and classifying distributed patterns of fMRI activity in human visual cortex,” *NeuroImage* **19**, 261–270 (2003).
3. J. T. Coull and A. C. Nobre, “Where and when to pay attention: the neural systems for directing attention to spatial locations and to time intervals as revealed by both PET and fMRI,” *J. Neurosci.* **18**, 7426–7435 (1998).
4. K. R. Pugh et al., “Auditory selective attention: an fMRI investigation,” *NeuroImage* **4**, 159–173 (1996).
5. K. L. Phan et al., “Functional neuroanatomy of emotion: a meta-analysis of emotion activation studies in PET and fMRI,” *NeuroImage* **16**, 331–348 (2002).
6. K. N. Ochsner et al., “Rethinking feelings: an fMRI study of the cognitive regulation of emotion,” *J. Cogn. Neurosci.* **14**(8), 1215–1229 (2002).
7. S. Koelsch et al., “Investigating emotion with music: an fMRI study,” *Hum. Brain Mapp.* **27**, 239–250 (2006).
8. A. E. Hernandez et al., “Language switching and language representation in Spanish-English bilinguals: an fMRI study,” *NeuroImage* **14**, 510–520 (2001).
9. M. P. van den Heuvel and H. E. Hulshoff Pol, “Exploring the brain network: a review on resting-state fMRI functional connectivity,” *Eur. Neuropsychopharmacol.* **20**, 519–534 (2010).
10. A. Orlichenko et al., “Latent similarity identifies important functional connections for phenotype prediction,” *IEEE Trans. Biomed. Eng.* **70**(6), 1979–1989 (2023).
11. W. Hu et al., “Deep collaborative learning with application to the study of multimodal brain development,” *IEEE Trans. Biomed. Eng.* **66**(12), 3346–3359 (2019).
12. S. Içer, İ. Acer, and A. Baş, “Gender-based functional connectivity differences in brain networks in childhood,” *Comput. Methods Programs Biomed.* **192**, 105444 (2020).
13. B. Sen and K. K. Parhi, “Predicting biological gender and intelligence from fMRI via dynamic functional connectivity,” *IEEE Trans. Biomed. Eng.* **68**(3), 815–825 (2021).
14. A. Orlichenko et al., “Imagenomer: description of a functional connectivity and omics analysis tool and case study identifying a race confound,” *NeuroImage Rep.* **3**, 100191 (2023).
15. S. Wang et al., “Abnormal long- and short-range functional connectivity in adolescent-onset schizophrenia patients: a resting-state fMRI study,” *Progr. Neuro-Psychopharmacol. Biol. Psychiatry* **81**, 445–451 (2018).
16. B. Rashid et al., “Classification of schizophrenia and bipolar patients using static and dynamic resting-state fMRI brain connectivity,” *NeuroImage* **134**, 645–657 (2016).
17. P. R. Millar et al., “Predicting brain age from functional connectivity in symptomatic and preclinical Alzheimer disease,” *NeuroImage* **256**, 119228 (2022).

18. G. Qu et al., “Ensemble manifold regularized multi-modal graph convolutional network for cognitive ability prediction,” *IEEE Trans. Biomed. Eng.* **68**, 3564–3573 (2021).
19. E. S. Finn et al., “Functional connectome fingerprinting: identifying individuals using patterns of brain connectivity,” *Nat. Neurosci.* **18**, 1664–1671 (2015).
20. B. Cai et al., “Refined measure of functional connectomes for improved identifiability and prediction,” *Hum. Brain Mapp.* **40**, 4843–4858 (2019).
21. A. Orlichenko et al., “Angle basis: a generative model and decomposition for functional connectivity,” (2023).
22. N. U. F. Dosenbach et al., “Prediction of individual brain maturity using fMRI,” *Science* **329**, 1358–1361 (2010).
23. L. E. Mak et al., “The default mode network in healthy individuals: a systematic review and meta-analysis,” *Brain Connect.* **7**, 25–33 (2017).
24. B. Ficek-Tani et al., “Sex differences in default mode network connectivity in healthy aging adults,” *Cereb. Cortex* **33**(10), 6139–6151 (2022).
25. A. M. Fjell et al., “Relationship between structural and functional connectivity change across the adult lifespan: a longitudinal investigation,” *Hum. Brain Mapp.* **38**, 561–573 (2017).
26. A. M. Staffaroni et al., “The longitudinal trajectory of default mode network connectivity in healthy older adults varies as a function of age and is associated with changes in episodic memory and processing speed,” *J. Neurosci.* **38**, 2809–2817 (2018).
27. S. Hirsiger et al., “Structural and functional connectivity in healthy aging: associations for cognition and motor behavior,” *Hum. Brain Mapp.* **37**, 855–867 (2016).
28. A. Salami et al., “Longitudinal evidence for dissociation of anterior and posterior MTL resting-state connectivity in aging: links to perfusion and memory,” *Cereb. Cortex* **26**, 3953–3963 (2016).
29. C. Sudlow et al., “UK Biobank: an open access resource for identifying the causes of a wide range of complex diseases of middle and old age,” *PloS Med.* **12**, e1001779 (2015).
30. S. M. Smith, F. Alfaro-Almagro, and K. L. Miller, “UK Biobank brain imaging documentation,” tech. rep., UK Biobank (2022).
31. A. R. Hariri et al., “The amygdala response to emotional stimuli: a comparison of faces and scenes,” *NeuroImage* **17**, 317–323 (2002).
32. F. Alfaro-Almagro et al., “Image processing and quality control for the first 10,000 brain imaging datasets from UK Biobank,” *NeuroImage* **166**, 400–424 (2018).
33. K. J. Friston, “Statistical parametric mapping,” in *Neurosci. Databases*, R. Kötter, Ed., pp. 237–250, Springer, Boston (2003).
34. J. D. Power et al., “Functional network organization of the human brain,” *Neuron* **72**, 665–678 (2011).
35. A. Orlichenko et al., “Identifiability in functional connectivity may unintentionally inflate prediction results,” (2023).
36. F. Pedregosa et al., “Scikit-learn: machine learning in Python,” *J. Mach. Learn. Res.* **12**, 2825–2830 (2011).
37. T. D. Satterthwaite et al., “Neuroimaging of the otterdamia neurodevelopmental cohort,” *NeuroImage* **86**, 544–553 (2014).
38. L. Farràs-Permanyer et al., “Age-related changes in resting-state functional connectivity in older adults,” *Neural Regen. Res.* **14**(9), 1544 (2019).
39. A. Hafkemeijer et al., “Increased functional connectivity and brain atrophy in elderly with subjective memory complaints,” *Brain Connect.* **3**, 353–362 (2013).
40. R. C. Petersen et al., “Alzheimer’s Disease Neuroimaging Initiative (ADNI): clinical characterization,” *Neurology* **74**, 201–209 (2010).
41. R. Sala-Llonch, D. Bartrés-Faz, and C. Junqué, “Reorganization of brain networks in aging: a review of functional connectivity studies,” *Front. Psychol.* **6**, 663 (2015).
42. B. Malagurski et al., “Longitudinal functional connectivity patterns of the default mode network in healthy older adults,” *NeuroImage* **259**, 119414 (2022).
43. H. I. Zonneveld et al., “Patterns of functional connectivity in an aging population: the otterdam study,” *NeuroImage* **189**, 432–444 (2019).
44. D. D. Jolles et al., “A comprehensive study of whole-brain functional connectivity in children and young adults,” *Cereb. Cortex* **21**, 385–391 (2011).

Anton Orlichenko received his BS degree in electrical and computer engineering in 2010 from the Illinois Institute of Technology. He is currently a PhD candidate at Tulane University, working on mathematical models of brain function and genetics.

Kuan-Jui Su received his PhD from Tulane University School of Medicine in 2023. He is currently employed at the Center for Biomedical Informatics and Genomics at Tulane University.

Hui Shen received his BS degree from the University of Science and Technology in China and his PhD from Creighton University. He is currently a geneticist at the Center for Biomedical Informatics and Genomics at Tulane University.

Hong-Wen Deng received his BS and MS degrees from Peking University. He received another MS degree and his PhD from the University of Oregon. He currently runs the Center for Biomedical Informatics and Genomics at the Tulane University School of Medicine.

Yu-Ping Wang received his BS degree from Tianjin University in 1990 and his MS degree and PhD from Xian Jiaotong University in 1993 and 1996, respectively. He currently runs the Multiscale Bioimaging and Bioinformatics Lab at Tulane University.